Asymptotic properties of bound states in coupled quantum wave guides

2006 J. Phys. A: Math. Gen. 39 1207

(http://iopscience.iop.org/0305-4470/39/5/013)

INSTITUTE OF PHYSICS PUBLISHING JOURNAL OF PHYSICS A: MATHEMATICAL AND GENERAL

J. Phys. A: Math. Gen. **39** (2006) 1207–1228 doi:10.1088/0305-4470/39/5/013

Asymptotic properties of bound states in coupled quantum wave guides

Enrico Maglione[1,2,3,4], **Lídia S Ferreira**[3,4] **and Giorgio Cattapan**[1,2]

[1] Dipartimento di Fisica G Galilei, Via F Marzolo 8, Padova, Italy
[2] Istituto Nazionale di Fisica Nucleare, Sezione di Padova, Italy
[3] Centro de Física das Interacções Fundamentais (CFIF), Avenida Rovisco Pais, Lisboa, Portugal
[4] Departamento de Física, Instituto Superior Técnico, Avenida Rovisco Pais, P1049-001 Lisboa, Portugal

E-mail: maglione@pd.infn.it

Received 1 September 2005, in final form 2 December 2005
Published 18 January 2006
Online at stacks.iop.org/JPhysA/39/1207

Abstract

We investigate the motion of bound-state poles in two quantum wave guides laterally coupled through a window. The imaginary momentum ik at the bound-state poles is studied as a function of the size a of the window. Both bound and virtual states appear as a spans the whole range from 0 up to $+\infty$. We are able to find simple scaling laws relating the critical value of the window size at which the nth bound state appears to the number n of bound states, in the limit of large n. A similar relation is also provided for the slope and the second derivative of the pole trajectories in the (k, a) plane. These relations are characterized by an extremely high numerical accuracy. We also evaluate the exact value of the first two derivatives for $a = 0$.

PACS numbers: 03.65.Ge, 73.21.−b

1. Introduction

With recent developments in microelectronics it is possible to create in the laboratory almost two-dimensional wave guides where the motion of the electrons can exhibit typical quantum effects [1–6]. These quantum wires are crystalline structures, characterized by high purity. At low temperatures, where electron–phonon and electron–electron scattering are negligible, the electron mean free path is large with respect to the wire size, and the electron achieves the ballistic regime and can be considered as a free particle. At the same time, the absence of inelastic processes assures phase coherence of the electron wavefunction, so that quantum interference phenomena become amenable to experimental investigation.

Mesoscopic systems of this type have received a lot of attention in recent times [7–10], since they allow us to study new physics, where the dual particle–wave nature of matter is exposed at a length scale between 100 Å and a few μm. The recent technological advances in

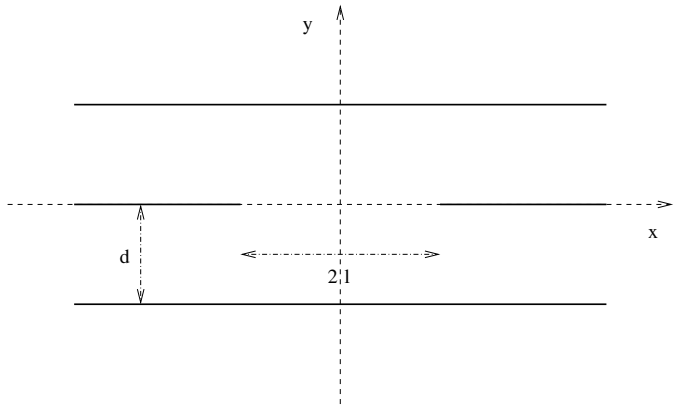

Figure 1. Two separate conducting strips of width d communicating through a common window of length $2l$.

semiconductors have succeeded in producing such devices. Experimental evidence is available of quantum interference phenomena in confined geometries, such as narrow constrictions [1, 2], quantum wires with a stub structure [3, 4] or with double-bend discontinuities [5, 6].

The strong analogies between quantum electronic systems and optical devices have been often stressed and have given major impetus to mesoscopic physics [8, 11]. This analogy stems from the close similarity between the stationary Schrödinger equation for the electron and the Maxwell equation for the electric field, as used in integrated optics [11]. Noteworthy examples of these similarities are provided by electron focusing through a mesoscopic electrostatic lens, and by Fabry-Pèrot-like transmission resonances in semiconductor superlattice structures [8].

The geometry of systems, such as bends, corners or crosses has a strong influence on the conduction properties of the electrons. This can be easily understood when conduction is regarded as a transport phenomenon, which in the mesoscopic domain is essentially determined by the scattering matrix of the device. When the proper boundary conditions are imposed on the solution of the Schrödinger equation, the behaviour of the wavefunction becomes sensitive to the shape of the device. As a consequence, pure geometric properties in conduction channels can lead to bound states or resonances. Therefore, it is quite important nowadays to have an accurate description of the relation between geometry and observables. This relation is highly implicit, since it emerges from the solution of a multichannel eigenvalue problem. To grasp the physics of mesoscopic devices, it is valuable to obtain simple, explicit relations between the shape of the system and its physical behaviour.

In the present work we consider two straight quantum wires of the same width, which can communicate through a window in their common boundary, as shown in figure 1, and study the behaviour of bound states when the window size is varied. This system can be considered as an idealized model of actual quantum-wire devices, such as the four-terminal electron waveguide coupler [12] or the quantum switch [13], and has been considered both theoretically [14] and experimentally [15] already several years ago. It turns out that the transport properties of coupled quantum wires reflect the spectral properties of the associated Hamiltonian with the proper boundary conditions. On physical grounds, the potential confining the electrons in the transverse direction ought to be evaluated self-consistently, leading to potential wells which in many cases are rather flat inside the guide, and increase rather steeply at the borders. A rigorous treatment of the problem with a finite potential well would imply the inclusion of the continuum in the basis functions, which is a very complex problem. Therefore, it is usual to introduce an idealized model for quantum wave guides, with hard wall (Dirichlet) boundary conditions.

Coupled quantum wave guides have been the subject of several detailed investigations in the literature [16–23], where bounds on the number of bound states and a corresponding scaling law with the window size were found. From the geometry of the problem, one expects a dependence upon only one parameter, such as the ratio a between the window size and the width of one of the wires. Problems of this type occur frequently in physics, where a has the meaning of strength of an interaction. Motivated by this analogy, we decided to apply well-established techniques of scattering theory, to analyse the motion of the S-matrix poles in the complex momentum plane. This allows one to follow the evolution of a bound state into a resonance as the 'strength' a is varied. In particular, we study the threshold region, where a new bound state is produced as the size parameter a increases, and provide an explicit functional relation between this critical value of a and the total number n of bound states supported by the system.

The trajectories described by the bound-state poles in the complex momentum plane exhibit an increasingly similar shape and slope with increasing a. Through a combination of analytical and numerical methods, we show that the slope approaches the asymptotic value $3\pi/4$; higher-order correction terms depend exponentially upon n and, consequently, upon the size parameter.

The behaviour of the second derivative of the trajectory is also studied, as well as the limiting case of $a = 0$.

This paper is organized as follows. In section 2, we briefly summarize the formalism for the bound-state problem. The analytical relation among the number n of bound states, and the critical value of the size parameter a, at which the nth bound state appears, is presented in section 3, in the limit of a very large window. There, we also discuss the asymptotic behaviour of the slope of the bound-state pole trajectories in the complex momentum plane.

2. The bound-state problem

Let us consider the system shown in figure 1, consisting of two symmetric wave guides of infinite length and width d, communicating through a window of width $2l$. When solving the multichannel problem, one generally exploits as much as possible the symmetry properties of the problem under consideration. In the present case, one takes into account the right–left mirror symmetry with respect to the centre of the window, plus the up–down symmetry with respect to the x-axis [16]. This implies for the bound and scattering wavefunctions, definite *parity* properties, under the transformation $x \leftrightarrow -x$ or $y \leftrightarrow -y$. The solutions antisymmetric with respect to the x-axis have to vanish at the window, so that the corresponding eigenspectrum is trivial, consisting of the eigenvalues of two separate strips, with no bound states, but only scattering states. For the solutions symmetric with respect to the x-axis, the left–right symmetry can be exhibited by resorting to wavefunctions with definite parity properties $\psi_{\pm}(x, y)$, where

$$\psi_{\pm}(x, y) = \pm\psi_{\pm}(-x, y). \tag{1}$$

As a consequence, one can limit oneself to solutions for $x \geqslant 0$ only, with the Dirichlet boundary condition that they vanish for $x = 0$ for odd $(-)$ parity, or the Neumann boundary condition implying the first derivative to vanish at the origin, for the even (+) case. Moreover, the up–down symmetry of the solutions implies that one can limit oneself to the first quadrant only, namely $x \geqslant 0, 0 \leqslant y \leqslant d$.

Due to the geometry of the problem, a particle propagating in the device is confined within the wires, and the wavefunction has to vanish along the walls, which corresponds to Dirichlet boundary conditions, except in the open window region of width $2l$. Consequently, the wave number in the transverse direction $k_{\perp}$ is quantized, leading to standing waves $\chi_j(y)$ in this

direction, which can be used as basis functions to expand the total wavefunction $\psi(x, y)$. In the following, we assume that there are N transverse modes in each duct.

In the outer region outside the window the bound-state wavefunction has to fulfil outgoing wave boundary conditions, in all channels, namely

$$\psi_{\pm}^{\text{out}}(x, y) = \sum_j \rho_j^{\pm} \exp\left[\mathrm{i}k_{\|j}(x - l)\right]\chi_j(y) \quad x \geqslant l \tag{2}$$

where the longitudinal wave number $k_{\|j}$ is a positive pure imaginary number for a bound state, implying the usual exponential decreasing behaviour for equation (2). The transverse eigenfunctions have the form

$$\chi_j(y) = \sqrt{\frac{2}{d}} \sin\left(j\frac{\pi}{d}y\right). \tag{3}$$

It is convenient to use the width of the wave guide as the basic scale parameter, and measure all quantities in relation to it. Thus, we use units such that $\hbar^2/2m = 1$, and express the total energy E in units of $(\pi/d)^2$. Separating the longitudinal and transverse motion one can write

$$E = k_{\perp j}^2 + k_{\|j}^2, \tag{4}$$

with the scattering region starting at $E = 1$. Bound states are located below the continuum threshold, and are contained in the energy interval $1/4 < E < 1$. The boundary conditions imply a quantization for the energy stored in the transverse modes in the form $k_{\perp j} = j$, with j a positive integer. Energy can be transferred from the longitudinal motion to the transverse modes. If m transverse modes ($1 \leqslant m \leqslant N$) can be excited because of energy conservation, one has in general m open channels or propagating modes, and $N - m$ closed channels (evanescent modes). For the latter, energy conservation implies that the longitudinal momenta $k_{\|j} = ik_j$ are purely imaginary, with k_j given by

$$k_j = \sqrt{j^2 - E}, \qquad j > m, \tag{5}$$

in units of π/d.

In the inner region ($0 \leqslant x \leqslant l, 0 \leqslant y \leqslant d$) the symmetric and antisymmetric wavefunctions are

$$\psi_{+}^{in}(x, y) = \sum_j b_j^{+} \frac{\cos(p_j x)}{\cos(p_j l)} \eta_j(y) \tag{6}$$

$$\psi_{-}^{in}(x, y) = \sum_j b_j^{-} \frac{\sin(p_j x)}{\sin(p_j l)} \eta_j(y), \tag{7}$$

where the transverse basis functions are

$$\eta_j(y) = \sqrt{\frac{2}{d}} \sin\left((2j - 1)\frac{\pi}{2d}(d - y)\right), \qquad j = 1, 2, \ldots. \tag{8}$$

Here, the up–down symmetry restricts the transverse quantum numbers to odd values $2j - 1$ only. The quantities p_j, due to energy conservation, have to fulfil $p_j = \sqrt{E - \left(j - \frac{1}{2}\right)^2}$.

The coefficients $\rho_j^{\pm}$ in equation (2), and $b_j^{\pm}$ in equations (6), (7) can be evaluated from the matching conditions at $x = l$ for the wavefunctions and their derivatives, with definite parity inside and outside the window,

$$\psi_{\pm}^{(\text{in})}(l, y) = \psi_{\pm}^{(\text{out})}(l, y), \qquad \left.\frac{\partial \psi_{\pm}^{(\text{in})}(x, y)}{\partial x}\right|_{x=l} = \left.\frac{\partial \psi_{\pm}^{(\text{out})}(x, y)}{\partial x}\right|_{x=l}, \tag{9}$$

where $\psi_{\pm}^{(\mathrm{in})}(x, y)$ and $\psi_{\pm}^{(\mathrm{out})}(x, y)$ are given by equations (6), (7) and (2), respectively. One finds [16]

$$\rho_j^{\pm} = \sum_m \langle \chi_j | \eta_m \rangle b_m^{\pm} \tag{10}$$

where the quantities $b_m^{\pm}$ are the solutions of the linear equations

$$\sum_m \left[k_j \mp Q_m^{\pm}(p_m l) \right] \langle \chi_j | \eta_m \rangle b_m^{\pm} = 0, \tag{11}$$

where the scalar products $O_{jm} \equiv \langle \chi_j | \eta_m \rangle$ can be evaluated analytically, and are given by

$$O_{jm} = (-1)^{m+1} \frac{2}{\pi} \frac{j}{j^2 - (m - 1/2)^2}, \tag{12}$$

and the functions $Q_m^{\pm}(p_m l)$ are defined according to

$$Q_m^{+}(p_m l) = p_m \tan(p_m l), \qquad Q_m^{-}(p_m l) = p_m \cot(p_m l). \tag{13}$$

It is worth noting that the coupling between the channels is here realized through the existence of specific boundary conditions imposed by geometry.

3. Bound states and their scaling properties

When a bound state occurs, the wavefunction is localized mainly inside the window, and there is no incoming wave. Under these circumstances all channels remain closed, and the homogeneous equations (11) have non-trivial solutions only if the determinant of the matrix

$$\mathcal{M}_{jm}^{\pm} = \left[k_j \mp Q_m^{\pm}(p_m l) \right] O_{jm} \tag{14}$$

vanishes. This gives the secular equation $\det \mathcal{M}^{\pm} = 0$, determining the purely imaginary channel momenta $\mathrm{i}k_j$. We solved the secular equation for different values of the size parameter $a = l/d$. Since for a given energy E, the momenta k_j are related to each other for the various values of j by equation (4), we have chosen the momentum associated with the lowest transverse mode k_1 as an independent variable, and determined how it behaves as a function of a. The reason for the choice of the momentum plane instead of the energy plane is twofold. As we shall see, the secular equation has solutions for both $k_1 > 0$ and $k_1 < 0$, in correspondence to bound and virtual states, respectively. The existence of virtual states is most easily exhibited in the complex momentum plane, whereas a careful analytic prolongation into the unphysical sheet would be required in the E plane. A second motivation for this choice stems from our requirements of numerical accuracy. The pole trajectories in the (k_1, a) plane are rather steep near the threshold value $k_1 = 0$. This is not the case in the energy plane, where the pole trajectories join smoothly the $E = 1$ axis, which could result in numerical instabilities near threshold, as already noted in [16].

In principle, the secular equation ought to be solved for an infinite number of basis functions; however, from a practical point of view, one has to resort to truncations. We checked the convergence of our calculations by locating the bound-state poles employing $N = 1, 2, 4, 8 \ldots$ up to $N = 2^{10} = 1024$ basis functions. We plot in figure 2 the energy E in units of $(\pi/d)^2$, as a function of the size parameter a, in correspondence to solutions of the secular equation for both the even and the odd cases. Both anti-bound and bound states occur according to the negative or positive sign, respectively, of k_1. They are represented in figure 2 by dashed and full lines, respectively. With the window closed, one has two separate strips, with a purely continuous spectrum, starting at $E = 1, k_1 = 0$. When the window opens up, a positive-parity bound state appears, that is $k_1 > 0$, starting from the upper edge

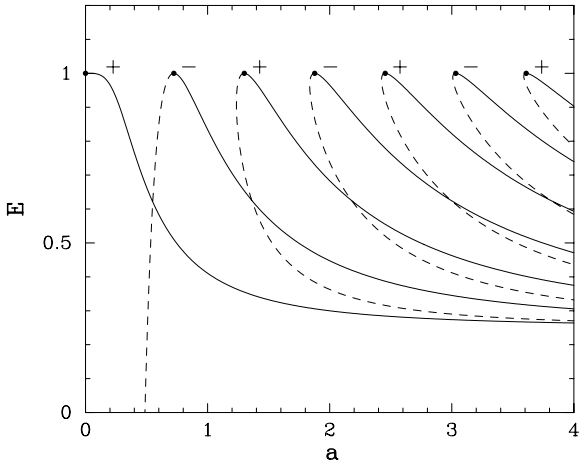

Figure 2. Energy of the positive (+) and negative (−) parity bound states as a function of the size parameter $a \equiv l/d$. Energies are given in terms of $(\pi/d)^2$, so that the threshold is fixed at $E = 1$. Both bound (full lines) and virtual (dashed lines) states appear as a varies.

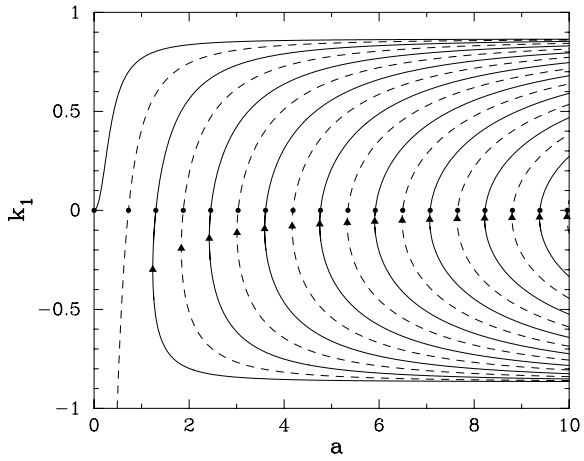

Figure 3. Motion of the bound-state poles in the complex momentum plane for varying a. The momentum ik_1 for the fundamental mode is plotted as a function of a. The full lines represent the positive parity poles, whereas the dashed lines refer to negative parity states. The triangles mark the points in the (k_1, a) plane where the virtual states evolving from a bound state, with decreasing a, collide with another virtual state. The full circles indicate the values of a for which a bound state appears at threshold.

of the bound-state region $E = 1$. The bound-state pole moves with increasing a towards the asymptotic limit of a single wire with width $2d$. This gives an energy $E = 1/4$, corresponding to the minimum energy available in the transverse mode, the associated closed-channel wave number being $k_1 = \sqrt{3}/2$. Note that $E = 1/4$ coincides with the lower edge of the energy interval where bound states may be located.

The role played by bound and virtual (or anti-bound) states can be more clearly perceived in figure 3, where the momentum k_1 at the poles is plotted as a function of a. The first odd solution appears as a virtual state in the lower k-plane, $k_1 < 0$. It is associated with

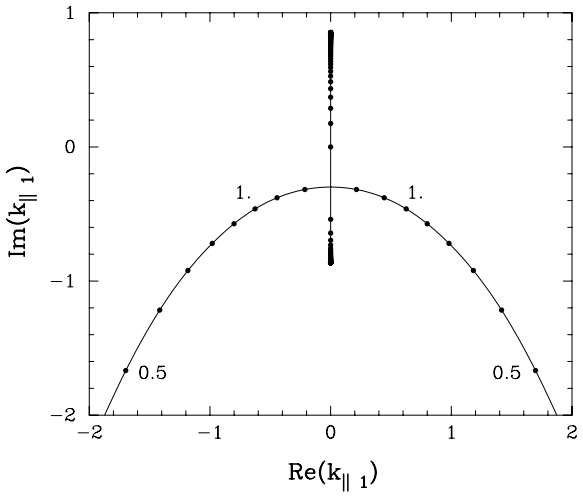

Figure 4. Motion of the poles associated with the second positive parity solution in the complex $k_{\|1}$-plane, with varying a. The dots correspond to values of a which differ by $\Delta a = 0.1$. As a decreases, the bound-state pole moves downwards, and the anti-bound state pole moves upwards along the imaginary axis. For $a < 1.3$ the two poles move downwards in the lower half-plane.

a wavefunction which grows exponentially as $x \to \pm\infty$. For $a \sim 0.7$ the solution of the secular equation changes sign, and one gets a bound-state pole moving upwards on the positive imaginary axis of the complex momentum plane. The following even and odd poles move along regular and equally spaced trajectories, in a quite symmetric fashion, their number increasing monotonically with the window width. From the numerical solution of the secular equation, one in general observes for a certain a several solutions, which can be grouped into pairs of a bound and an anti-bound state. They tend to gather near the asymptotic momentum values $\pm\sqrt{3}/2$, corresponding to a unique wave guide of width $2d$. With decreasing a, the bound and virtual states of each pair will move towards each other, colliding at a certain point shown in the figure by a triangle. As in potential scattering theory, this point corresponds to the threshold where a resonance and an anti-resonance appear, moving away in opposite directions of the complex k-plane. This is illustrated in figure 4 for the second even solution. For large a, as a decreases, the poles associated with the bound and anti-bound states move slowly towards each other on the imaginary k-axis, in correspondence to the flat part of the trajectory in the (k_1, a) plane of figure 3. As the slope of the trajectory increases, the two poles move faster on the imaginary axis, and collide for $a \simeq 1.3$, at $k_1 \simeq -0.3$. For decreasing a, they move in the lower complex momentum plane with increasing velocity, along trajectories symmetric with respect to the imaginary axis. As is well-known, the pole in the fourth quadrant corresponds to a resonance, whereas the pole in the third quadrant represents an anti-resonance. The collision points in the (k_1, a) plane approach the $k_1 = 0$ value for very large a, as can be seen in figure 3.

The existence of bound states for this type of wave guides has been already proved in [16], where bounds on their number with varying a, and on the critical values of the window width at which they appear have been provided. We have decided to perform a few computer experiments, in order to have a deeper insight into the behaviour of the bound states for varying a. To this end, particular care has been taken with the numerical accuracy of the calculations. It was found that, employing $N = 1, 2, 4, \ldots$ up to $N = 2^{10}$ basis functions, at each step the difference between the new estimate of a and the previous one was almost halved, so that a

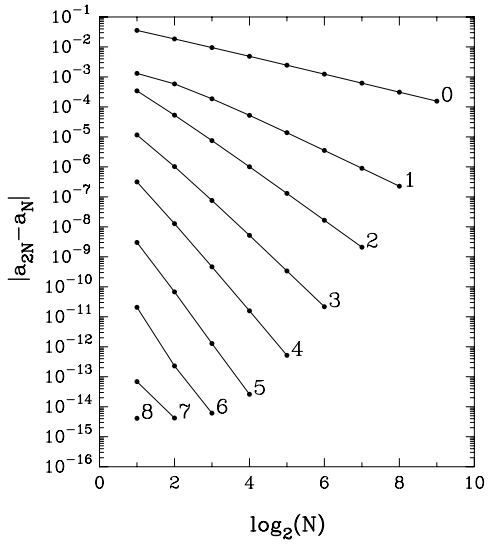

Figure 5. The increase of convergence attained through repeated application of the Richardson extrapolation method. For each step of the procedure ($s = 0, 1, 2, \ldots, 8$), the full dots give the quantities $|a_{2N}^{(s)} - a_N^{(s)}|$ as a function of $\log_2 N$, where N represents the dimension of the basis. The full lines are only for illustrative purpose.

relation of the form

$$a_c = a_N + \frac{\alpha}{N^p} + \mathcal{O}\left(\frac{1}{N^{p+1}}\right), \tag{15}$$

with $p = 1$, can be assumed between the converged value a_c and the Nth order estimate a_N. Convergence can be improved by applying the Richardson extrapolation method [24]. Considering equation (15) for N and $2N$, and eliminating the constant α, one has the new series of approximations $a_N^{(1)}$, which also satisfy equation (15), but with $p = 2$. Repeating this procedure, one has at the sth step

$$a_N^{(s)} = \frac{2^p a_{2N}^{(s-1)} - a_N^{(s-1)}}{2^p - 1}, \qquad s = 1, 2, \ldots \tag{16}$$

which ought to fulfil equation (15) with $p = 1 + s$. In figure 5 we report the result of repeated applications of Richardson procedure. The deviations $\left|a_{2N}^{(s)} - a_N^{(s)}\right|$ are plotted for each step as a function of the logarithm of N in base 2. The dots on the top line represent the results obtained varying N up to $N = 2^{10}$ basis functions, whereas the dots on the other lines give the deviations obtained with successive applications of the Richardson method. The results lie on almost straight lines of increasing slope for each calculation, exhibiting the increasing convergence of the series. The almost linear dependence in figure 5 implies that $\left|a_{2N}^{(s)} - a_N^{(s)}\right|$ scales as a power of N. Actually, it was found that, with 2^{10} basis functions, at the 6th step of the Richardson procedure, the accuracy of the calculations can be guaranteed up to the 14th significant digit. Such computer experiments are relevant for the present work, which aims at fixing the asymptotic behaviour of the bound state solutions with a high degree of accuracy.

In figure 6(*a*) we plot the critical value a_n of the size parameter, at which the nth bound state appears, as a function of the number n of bound states. The quantity a_n ought to fulfil the bounds (2.6) of [16], which in our notation reads for symmetric guides $(n-1)\sqrt{3} \leqslant a_n \leqslant n\sqrt{3}$. Figure 6(*a*) is consistent with this result, and exhibits a clear linear dependence of a_n

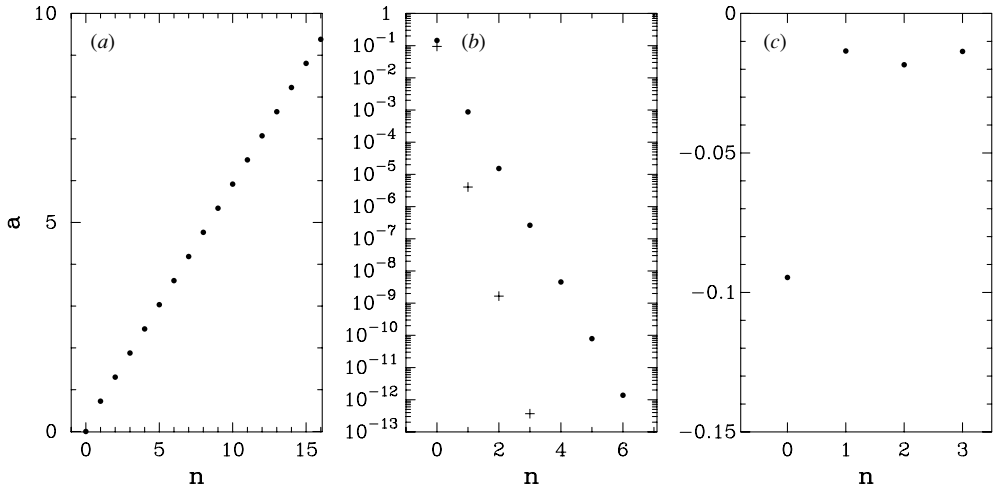

Figure 6. (*a*) Critical values of the size parameter a at which a new bound state appears as functions of the number of bound states n. (*b*) Absolute value of the difference between the outcome of the numerical calculation and the values given by the first two (full dots) and three (crosses) terms in the asymptotic formula (28), on a log scale. (*c*) Difference between the outcome of the numerical calculation and the values given by the first three terms in the asymptotic formula (28), divided by $\exp(-2\sqrt{5/3}\pi n)$.

upon n. Similarly, one immediately verifies that our results agree with the inequality $a_n\sqrt{3} \leqslant n \leqslant 1 + a_n\sqrt{3}$, for the number of bound states supported by a window of given width [16].

From the previous discussion, it seems that there is an almost linear dependence of the number of bound states on a. To have a deeper understanding of the physical properties of the mesoscopic devices considered here, it is quite interesting to ascertain how the appearance of bound states depends upon the length parameter a. The asymptotic behaviour of the bound state eigenvalues at threshold has been the subject of several mathematical investigations in recent times [19, 20]. Here, we approach a similar question, looking for explicit and accurate functional relations between the critical value of a at which a new bound state emerges from the continuum, and the number n of bound states.

First, we observe that the matrix $\mathcal{M}^{\pm}_{jm}$ can be rewritten as

$$\mathcal{M}^{\pm}_{jm} = (-1)^{m+1}\frac{2j}{\pi^2}A^{\pm}_{jm}. \tag{17}$$

The reduced matrix $A^{\pm}_{jm}$ is given by

$$A^{\pm}_{jm} = \left[\pi\sqrt{j^2 - 1 + k_1^2} \mp \pi\sqrt{1 - k_1^2 - (m-1/2)^2}\, f^{\pm}_m\right] o_{jm}, \tag{18}$$

where

$$f^{+}_m(k_1, a) \equiv \tan\left(\pi\sqrt{1 - k_1^2 - (m-1/2)^2}\, a\right) \tag{19}$$

$$f^{-}_m(k_1, a) \equiv \cot\left(\pi\sqrt{1 - k_1^2 - (m-1/2)^2}\, a\right), \tag{20}$$

$$o_{jm} \equiv \frac{1}{j^2 - (m-1/2)^2}, \tag{21}$$

and momenta are measured in terms of π/d. One can easily verify that for a matrix of the form $S_{ij} = \alpha_i \beta_j s_{ij}$, like the one under consideration, one has $\det S = \det s \prod_{i=1}^{N} \alpha_i \beta_i$. Since we have to solve the secular equation $\det \mathcal{M}^{\pm} = 0$, we shall from now on refer to the simpler matrix A. Moreover, we are interested in the situation, when a new bound state appears at threshold, namely for $k_1 = 0$, so that the matrix A becomes simply

$$A^{\pm}_{jm}(k_1 = 0) = \left[u_j \mp z_m f^{\pm}_m(0, a)\right] o_{jm}, \tag{22}$$

with

$$u_j \equiv \pi\sqrt{j^2 - 1} \qquad z_m \equiv \pi\sqrt{1 - (m - 1/2)^2}. \tag{23}$$

and

$$f^{+}_m(0, a) \equiv \tan(z_m a) \tag{24}$$

$$f^{-}_m(0, a) \equiv \cot(z_m a), \tag{25}$$

For dimension 1 the result is trivial: for the symmetric solution the condition $\det A^{+} = 0$ leads immediately to

$$(\sqrt{3/4}\pi a) = \arctan(0) = n\pi \tag{26}$$

fulfilled by

$$a_n = \frac{2n}{\sqrt{3}} \qquad n = 0, 1, 2, \ldots \tag{27}$$

In the general case of larger dimensions, we are in presence of a nonlinear problem, since the width of the window and the number of bound states are related to each other through the secular equation. We solve the latter equation, using a truncated series expansion in non-integer powers of $\exp(-a)$. The calculation is very involved, and therefore was left to appendix A. In the limit of a large size parameter, and using the Richardson extrapolation method, we obtain for both the symmetric and the antisymmetric solutions

$$a^{\pm}_n \simeq \frac{n}{\sqrt{3}} + 0.145\,294\,477\,864\,05(1) \mp 0.050\,640\,518\,625\,32(1) \exp\left(-\sqrt{\frac{5}{3}}\pi n\right) + \mathcal{O}\left(\exp\left(-2\sqrt{\frac{5}{3}}\pi n\right)\right) \qquad n = 0, 1, 2, \ldots \tag{28}$$

where n is even (odd) for the symmetric (antisymmetric) case.

These expressions are confirmed by an inspection of figures 6(*b*) and (*c*). In figure 6(*b*) the difference between the numerical results and the calculation using only the first two or three terms of the asymptotic expression of equation (28) are shown on a log scale. They actually follow an exponential law, and are indistinguishable from the numerical noise beyond the fourth bound state. Figure 6(*c*) shows that higher order corrections in equation (28) behave as $\exp\left(-2\sqrt{\frac{5}{3}}\pi n\right)$. The oscillatory behaviour originates from the fact that higher order terms are different in the case of even and odd solutions.

As figure 3 shows, the trajectories of the bound- or virtual-state poles in the (k_1, a) plane exhibit an increasingly similar shape, and tend to cross the real axis with the same slope with increasing a. One may wonder whether there is some simple asymptotic law for the pole position underlying this geometric behaviour. The asymptotic properties of the bound state eigenvalues near the critical points a_n, where a new bound state emerges from the continuum, have been investigated in [19] under a mathematical point of view. There, it has been proven that the eigenvalues scale as $(a - a_n)^2$. It can be expected, therefore, that k_1 is a linear function

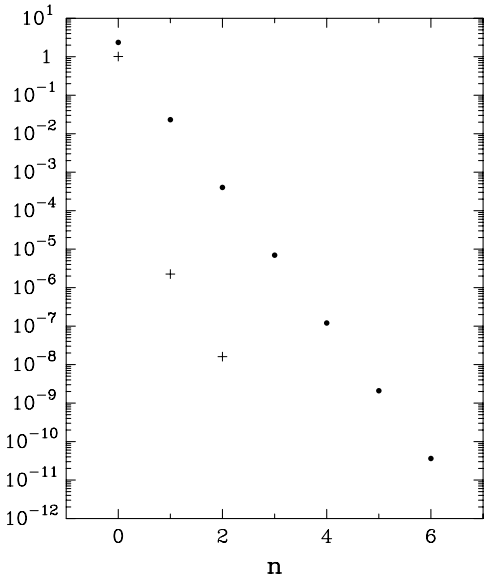

Figure 7. Absolute value of the difference between dk_1/da and the asymptotic value $(3/4)\pi$ (dots), and the first two terms of equation (30) (crosses), as a function of the number of bound states n.

of a in the neighbourhood of a_n, and that its first derivative approaches a constant value as $a \to \infty$, when higher-order correction terms are neglected. We shall show in the following that this is actually the case, providing the precise value of the leading term in the asymptotic expression of dk_1/da. To this end, one has to study the above derivative at $k_1 = 0$. Since the relation between k_1 and a is an implicit one, through the secular equation $\det A^{\pm} = 0$, the derivative has to be evaluated according to

$$\frac{dk_1}{da} = -\frac{\partial \det A^{\pm}}{\partial a} \Big/ \frac{\partial \det A^{\pm}}{\partial k_1}, \tag{29}$$

evaluated at $k_1 = 0$ and $a = a_n$. Details for the calculation of these derivatives are given in appendix B where we show that

$$\left(\frac{dk_1}{da}\right)_{k_1=0} = \frac{3}{4}\pi \mp 1.341\,109\,189\,5071(1) \exp\left(-\pi\sqrt{\frac{5}{3}}n\right) + \mathcal{O}\left(\exp\left(-2\sqrt{\frac{5}{3}}\pi n\right)\right). \tag{30}$$

The sign $\mp$ refers to the even and odd solutions, respectively, and, as usual, n runs over even or odd values, for the symmetric or antisymmetric case. One sees from equation (30) that the higher-order correction term decreases exponentially for large n, and the slope dk_1/da approaches the constant value $3\pi/4$. This behaviour is confirmed by a comparison with the outcome of numerical calculations, as shown in figure 7, where the quantity $|(dk_1/da)_{k_1=0} - 3\pi/4|$ is plotted for the first seven bound states. The linear dependence confirms the exponential behaviour exhibited in equation (30). Including also in the previous difference the second term of equation (30), the agreement is even better.

Proceeding in a similar way, the second derivative of k_1 with respect to a can be obtained, as described in appendix C, giving

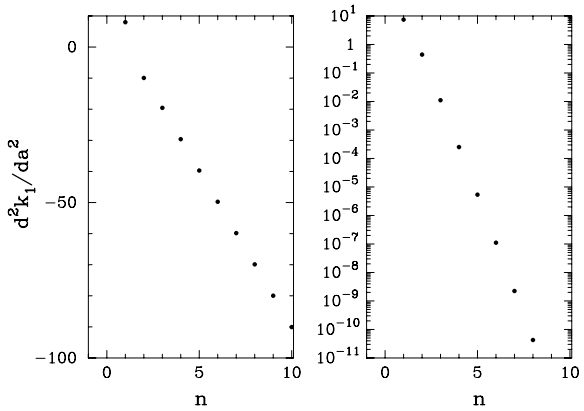

Figure 8. Second derivative of k_1 with respect to a (left panel), and absolute value of the difference between the second derivative and the first two terms of equation (31) (right panel), as a function of the number of bound states n.

$$\left(\frac{d^2k_1}{da^2}\right)_{k_1=0} = -\frac{3}{16}\sqrt{3}\pi^3 n + 0.577\,482\,652\,977\,66(1) + \mathcal{O}\left(\exp\left(-\pi\sqrt{\frac{5}{3}}n\right)\right),$$
$$n = 0, 1, 2, \ldots \tag{31}$$

valid for an infinite set of basis functions and large a.

The results of the numerical calculation of the second derivative are shown in figure 8, confirming the leading term and the exponential behaviour of higher order corrections, given by equation (31). It is worth noting that the leading term in equations (28, 30, 31) coincides with the analytic result one obtains restricting the dimension of the matrix $A^{\pm}$ to one.

We have considered also the behaviour of the first two derivatives of k_1 with respect to a at the origin $a = 0$. As detailed in appendices B and C, we found that the first derivative vanishes, while the second derivative is simply 8.

4. Conclusions

We have considered the bound states supported by two conducting strips communicating through a common window. Our analysis in the complex momentum plane has put in evidence the existence of both bound and virtual states, corresponding to solutions with a positive or negative coefficient of the imaginary momentum ik_1, respectively. We have considered in particular detail the behaviour of the bound-state poles for large values of the window size parameter $a \equiv l/d$. In the asymptotic regime the critical value of a at which a new bound state appears scales linearly with the number of supported bound states, in agreement with the analysis of [16]. In addition, we could provide a next-to-leading-order correction term, which decreases exponentially with n, as exhibited in equation (28). This term has been determined through a high-precision numerical analysis. We considered also the slope of the pole trajectories in the (k_1, a) plane at threshold. Again, our results are quite consistent with those of the previous mathematical analysis in the energy plane [19]. We found that, as a increases, dk_1/da approaches the simple value $(3/4)\pi$, the first correction term again decreasing exponentially as a function of n (see equation (30)). On the grounds of our computations, one may conclude that the asymptotic regime, described by the leading-order terms, is already reached beyond the fifth bound state. A similar study was done for the second

derivative of the trajectory, and for the limiting case of $a = 0$, for which the first derivative vanishes and the second derivative is simply equal to 8.

Acknowlegments

This work was supported by the Fundação de Ciência e Tecnologia (Portugal), Project: POCTI/FNU/44958/2002 and FEDER.

Appendix A

We are interested in determining at which value of the size parameter, a bound state appears, and obtain the functional dependence of a upon the total number n of existing bound states. The study will be made for the symmetric case, since anti-symmetric states can be dealt with in a similar fashion.

A bound state is defined by the condition that the determinant of the matrix defined by equation (18) vanishes,

$$\det A^{+}(k_1, a) = 0. \tag{A.1}$$

The threshold for the appearance of a bound state corresponds to the longitudinal momentum associated with the lowest transverse mode, $k_1 = 0$. At this momentum, the matrix $A^{+}(0, a)$ is given by equation (22), and it is immediate to see that $a = 0$ is a solution of equation (A.1), since the first row is identically zero. This implies that even the tiniest opening will create the conditions for the existence of a bound state.

To evaluate the non-vanishing values of the size parameter at which a new bound state appears, one has to solve equation (A.1). An analytic solution of this problem is clearly impossible; however, for very large a one can look for an approximate solution through a series expansion. To this end, we observe that the argument of the trigonometric functions in A_{jm} becomes for $m \geqslant 2$ a pure imaginary number $\mathrm{i}\alpha = \mathrm{i}\pi\sqrt{(m - 1/2)^2 - 1}\, a$, so that for $\alpha \to \infty$ one can resort to the series expansion

$$\tan(\mathrm{i}\alpha) = \frac{\mathrm{i}(\mathrm{e}^{2\alpha} - 1)}{(\mathrm{e}^{2\alpha} + 1)} = \mathrm{i}(1 - 2\mathrm{e}^{-2\alpha} + 2\mathrm{e}^{-4\alpha} + \mathcal{O}(\mathrm{e}^{-6\alpha})). \tag{A.2}$$

For a, and consequently α, large, we can keep only the first term $\tan(\mathrm{i}\alpha) \simeq \mathrm{i}$, and the matrix elements become

$$A^{+}_{j,1} = \left(\pi\sqrt{\mathrm{i}^2 - 1} - \pi\sqrt{\frac{3}{4}}\tan\left(\pi\sqrt{\frac{3}{4}}a\right)\right) o_{j,1} \tag{A.3}$$

$$A^{+}_{j,m} = (\pi\sqrt{\mathrm{i}^2 - 1} + \pi\sqrt{(j - 1/2)^2 - 1}) o_{j,m} \qquad j \geqslant 2 \tag{A.4}$$

that leads to the general solutions

$$a_n = \frac{2n}{\sqrt{3}} + \frac{2}{\pi\sqrt{3}}\arctan\left(\frac{2}{\pi\sqrt{3}}\frac{\det B}{\det C}\right) \qquad n = 0, 1, 2, \ldots \tag{A.5}$$

where the matrices B and C do not depend on a and are given by

$$B_{j1} = u_j o_{j1}, \qquad B_{jm} = (u_j + w_m) o_{jm} \qquad m > 1 \tag{A.6}$$

$$C_{j1} = o_{j1}, \qquad C_{jm} = (u_j + w_m) o_{jm} \qquad m > 1, \tag{A.7}$$

where u_j and o_{jm} are defined by equations (23) and (21), respectively, and

$$w_m \equiv \pi\sqrt{\left(m-\frac{1}{2}\right)^2-1}. \tag{A.8}$$

We note that, since the second term in the solution for large a, equation (A.5), does not depend on the number of bound states n, they will be equidistant from each other.

An improved estimate for a_n with respect to equation (A.5) can be obtained, keeping the exact expression (A.3) for A_{j1}, and including the second term in the series expansion of $\tan(\mathrm{i}\alpha)$ in the second column of A. This is justified since the smallest value of α is obtained for $m=2, \alpha=\pi\sqrt{\frac{5}{4}}a$. One obtains

$$A^+_{j2} = \left[u_j + \sqrt{\frac{5}{4}}\pi(1-2\mathrm{e}^{-\sqrt{5}\pi a})\right] o_{j2} \tag{A.9}$$

$$A^+_{jm} = (u_j + w_m)o_{jm}, \qquad m>2. \tag{A.10}$$

The equation we get now is

$$\det A^+ = \det B - \sqrt{\frac{3}{4}}\pi\tan\left(\sqrt{\frac{3}{4}}\pi a\right)\det C - \pi\sqrt{5}\mathrm{e}^{-\pi\sqrt{5}a} \times\left[\det D - \sqrt{\frac{3}{4}}\pi\tan\left(\sqrt{\frac{3}{4}}\pi a\right)\det E\right] = 0, \tag{A.11}$$

with

$$D_{j1} = u_j o_{j1}, \qquad D_{j2} = o_{j2}, \qquad E_{j1} = o_{j1}, \qquad E_{j2} = o_{j2}, \tag{A.12}$$

and $D_{jm} = E_{jm} = (u_j + w_m)o_{jm}$ for $m>2$.

Equation (A.11) can be solved only perturbatively, using as a starting value the approximation (A.5). We look for a solution of the form

$$a_n = \frac{2n}{\sqrt{3}} + \frac{2}{\pi\sqrt{3}}\arctan\left(\frac{2}{\sqrt{3}\pi}\frac{\det B}{\det C}\right) + x, \tag{A.13}$$

where x should be a small number. Substituting equation (A.13) into equation (A.11), and making a series expansion in x up to the first order we get

$$x = \frac{\sqrt{5}(\det B\det E - \det D\det C)}{\pi\left(\frac{3}{4}(\det C)^2 + \frac{1}{\pi^2}(\det B)^2\right)}\exp\left(-2\sqrt{\frac{5}{3}}\arctan\left(\frac{2}{\sqrt{3}\pi}\frac{\det B}{\det C}\right)\right)\exp\left(-2\sqrt{\frac{5}{3}}\pi n\right). \tag{A.14}$$

Using the Richardson extrapolation method to obtain a good approximation for the determinants of the matrices B, C, D, E, for very large N, we get

$$a_n = \frac{2n}{\sqrt{3}} + 0.145\,294\,477\,864\,05(1) - 0.050\,640\,518\,625\,32(1)\exp\left(-2\sqrt{\frac{5}{3}}\pi n\right) + \mathcal{O}\left(\exp\left(-4\sqrt{\frac{5}{3}}\pi n\right)\right) \qquad n=0,1,2,\ldots. \tag{A.15}$$

It is interesting to observe that, if only one transverse mode is considered, the matrix has dimension one, and the bound-state condition at threshold becomes simply

$$A^+_{11}(0,a) = -\sqrt{\frac{4}{3}}\pi\tan\left(\sqrt{\frac{3}{4}}\pi a\right) = 0 \tag{A.16}$$

which can be solved analytically, giving the leading term $a=\frac{2n}{\sqrt{3}}$ of equation (A.15).

The above arguments can be readily extended to the antisymmetric case, the only difference being the substitution of the function $\tan(z_m a)$ with $-\cot(z_m a)$. A calculation similar to the previous one gives

$$a_n \simeq \frac{2n+1}{\sqrt{3}} + \frac{2}{\pi\sqrt{3}}\arctan\left(\frac{2}{\sqrt{3}\pi}\frac{\det B}{\det C}\right) - \frac{\sqrt{5}(\det B \det E - \det D \det C)}{\pi\left(\frac{3}{4}(\det C)^2 + \frac{1}{\pi^2}(\det B)^2\right)} \times \exp\left(-2\sqrt{\frac{5}{3}}\arctan\left(\frac{2}{\sqrt{3}\pi}\frac{\det B}{\det C}\right)\right)\exp\left(-\sqrt{\frac{5}{3}}\pi(2n+1)\right) + \mathcal{O}\left(\exp\left(-2\sqrt{\frac{5}{3}}\pi(2n+1)\right)\right) \qquad n = 0, 1, 2, \ldots. \tag{A.17}$$

The above results can be summarized as follows,

$$a_n^{\pm} \simeq \frac{n}{\sqrt{3}} + 0.145\,294\,477\,864\,05(1) \mp 0.050\,640\,518\,625\,32(1)\exp\left(-\sqrt{\frac{5}{3}}\pi n\right) + \mathcal{O}\left(\exp\left(-2\sqrt{\frac{5}{3}}\pi n\right)\right) \qquad n = 0, 1, 2, \ldots \tag{A.18}$$

where even/odd n correspond to even/odd solutions, respectively.

Appendix B

In this appendix, the derivative of k_1 with respect to the size parameter (see equation (29)) is calculated at threshold, at the values of a where a bound state appears.

From the properties of determinants, the derivative of $\det A^{\pm}$ can be rewritten as a sum of N determinants, in which one row (or column) is substituted by the derivative of the matrix elements. Starting with the denominator of equation (29), noting that

$$\left.\frac{\partial A^{\pm}_{jm}}{\partial k_1}\right|_{k_1=0} = \pi\delta_{j1}o_{1m}, \tag{B.1}$$

only the first term of the sum is different from zero, and one gets

$$\frac{\partial \det A^{\pm}}{\partial k_1} = \det\left\|\left(\pi\delta_{j1} + (1-\delta_{j1})\left(u_j \mp z_m f_m^{\pm}\right)\right)o_{jm}\right\|, \tag{B.2}$$

with u_j and z_m given by equation (23). Here and in the following all the derivatives are evaluated at $k_1 = 0$.

The derivative of $\det A^{\pm}$ with respect to a, on the other hand, is the sum of N terms

$$\frac{\partial \det A^{\pm}}{\partial a} = \sum_{l=1}^{N} \det G^{(l)} \tag{B.3}$$

where

$$G^{(l)}_{jl} = \frac{\partial A^{\pm}_{jl}}{\partial a}, \qquad G^{(l)}_{jm} = A^{\pm}_{jm} \qquad m \neq l. \tag{B.4}$$

In the case of dimension 1, the above expressions can be easily evaluated giving

$$\frac{\partial \det A^{\pm}}{\partial k_1} = \frac{4}{3}\pi \tag{B.5}$$

and

$$\frac{\partial \det A^{\pm}}{\partial a} = -\pi^2 - \left(f_1^{\pm}\right)^2. \tag{B.6}$$

Since we have to calculate this function for the critical values $a = 2n/\sqrt{3}$ and $a = (2n+1)/\sqrt{3}$ in the symmetric and antisymmetric cases respectively, we get $\left(f_1^{\pm}\right)^2 = 0$, so that

$$\frac{\mathrm{d}k_1}{\mathrm{d}a} = \frac{3}{4}\pi. \tag{B.7}$$

We will see below that this result is the leading term of the derivative when the matrix has dimension N.

For larger dimensions, we should use the various approximations developed in appendix A not only to obtain the matrix A, but also for the dependence of a on the number of bound states. If we restrict ourselves to the first term in the expansion of $\tan(\mathrm{i}\alpha)$, one may use equation (A.5) for the size parameter. Since the derivative of A with respect to a is

$$\frac{\partial A^{\pm}_{jm}}{\partial a} = -z_m^2\left(1 + f_m^{\pm 2}(k_1, a)\right)o_{jm}, \tag{B.8}$$

one has the approximate expression

$$\frac{\partial A^{\pm}_{jm}}{\partial a} = 0 \qquad m > 1. \tag{B.9}$$

Thus, in equation (B.3) only the first term in the sum survives, and one may write

$$\frac{\mathrm{d}k_1}{\mathrm{d}a} = -\frac{\det G_0^1}{\det F_0} \tag{B.10}$$

with

$$\begin{aligned} \left(G_0^1\right)_{j1} &= -\left(\frac{3}{4}\pi^2 + \left(\frac{\det B}{\det C}\right)^2\right)o_{j1} \\ \left(G_0^1\right)_{jm} &= (u_j + w_m)o_{jm} \quad m > 1, \end{aligned} \tag{B.11}$$

and the matrix F_0 has elements in the first row of the form $(F_0)_{1m} = \pi o_{1m}$, and on the other rows ($j > 1$),

$$(F_0)_{j1} = \left(u_j - \frac{\det B}{\det C}\right)o_{j1}, \qquad (F_0)_{jm} = (u_j + w_m)o_{jm} \quad m > 1. \tag{B.12}$$

One can verify that

$$\frac{\mathrm{d}k_1}{\mathrm{d}a} = \frac{3}{4}\pi \tag{B.13}$$

whatever the dimension of the matrix $A^{\pm}$ is.

The higher-order contribution to the leading term (B.13) can be determined through a procedure similar to what has been done in the previous section. We refer to the symmetric case for the sake of simplicity. One inserts the estimate for a given by equations (A.13) and (A.14) into equation (B.2) for the partial derivative $\partial \det A^{+}/\partial k_1$, and retains only terms up to $\exp(-2\pi\sqrt{5/3}n)$. As for the derivative with respect to a, one has extra terms in the sum (B.3), because the first term acquires a higher-order contribution, and the second term is no longer equal to zero. Again, a series expansion truncated at next-to-leading order yields the correction term to $\mathrm{d}k_1/\mathrm{d}a$ as a function of the number of bound states n. Here, we limit

ourselves to quoting the extrapolated numerical result which, for both even and odd solutions, is given by

$$\left(\frac{\mathrm{d}k_1}{\mathrm{d}a}\right)_{k_1=0} = \frac{3}{4}\pi \mp 1.341\,109\,189\,507\,099\,014\,0286(1)\exp\left(-\pi\sqrt{\frac{5}{3}}n\right) + \mathcal{O}\left(\exp\left(-2\sqrt{\frac{5}{3}}\pi n\right)\right). \tag{B.14}$$

To complete this appendix, we have to evaluate the derivatives of k_1 at threshold where both k_1 and a are equal to zero. As we have seen from equation (29), this derivative is the ratio of derivatives of $\det A^+$. For $a = 0$, equation (B.2) reduces to

$$\frac{\partial \det A^+}{\partial k_1} = \det \|\pi(\delta_{j,1} + (1-\delta_{j,1})\sqrt{j^2-1})o_{jm}\|. \tag{B.15}$$

It can be shown that

$$\left(\frac{\partial \det A}{\partial k_1}\right)_{a=0} = \pi^N \left[\prod_{i=2,N}\sqrt{i^2-1}\right]\det O \tag{B.16}$$

where N is the dimension of the matrix and the matrix O is the matrix of the overlaps $o_{j,m}$.

Noting that

$$\prod_{i=2,N}\sqrt{i^2-1} = N!\sqrt{\frac{N+1}{2N}} \tag{B.17}$$

and that

$$\det O = \frac{4^{N^2}}{N!}\prod_{t=1,N}\frac{(2t-1)!^2}{(4t-1)!!(4t-3)!!} \tag{B.18}$$

we obtain

$$\left(\frac{\partial \det A}{\partial k_1}\right)_{a=0} = \pi^N 4^{N^2}\sqrt{\frac{N+1}{2N}}\prod_{t=1,N}\frac{(2t-1)!^2}{(4t-1)!!(4t-3)!!}. \tag{B.19}$$

Analogously, the derivative of $\det A$ with respect to a at threshold, and for $a = 0$, reduces to

$$\left(\frac{\partial \det A}{\partial a}\right)_{a=0} = \det \|\pi(\delta_{j,1}(-\pi(1-(m-1/2)^2)) + (1-\delta_{j,1})\sqrt{j^2-1})o_{j,m}\| \tag{B.20}$$

and we obtain

$$\left(\frac{\partial \det A}{\partial a}\right)_{a=0} = -\pi^{N+1}\left[\prod_{i=2,N}\sqrt{i^2-1}\right]\det \mathcal{O} = -\pi^{N+1}N!\sqrt{\frac{N+1}{2N}}\det \mathcal{O} \tag{B.21}$$

with

$$\mathcal{O}_{j,m} = \delta_{j,1} + (1-\delta_{j,1})o_{j,m}. \tag{B.22}$$

It can be shown that

$$\det \mathcal{O} = \frac{(2N+1)!((2N-3)!!)^2 4^{N^2-N}}{(N!)^2(N+1)!(2N-2)!}\prod_{t=1,N}\frac{(2t-1)!^2}{(4t-1)!!(4t-3)!!} \tag{B.23}$$

that leads to the final result

$$\left(\frac{\partial \det A}{\partial a}\right)_{a=0} = -\pi^{N+1}\frac{(2N+1)!((2N-3)!!)^2 4^{N^2-N}}{N!(N+1)!(2N-2)!}\sqrt{\frac{N+1}{2N}}\prod_{t=1,N}\frac{(2t-1)!^2}{(4t-1)!!(4t-3)!!}. \tag{B.24}$$

Using the expressions obtained in equations (B.19) and (B.24), we obtain the first derivative of k_1 with respect to a, for $a = 0$,

$$\left(\frac{\mathrm{d}k_1}{\mathrm{d}a}\right)_{a=0} = -\frac{\frac{\partial \det A}{\partial a}}{\frac{\partial \det A}{\partial k_1}} = \pi\frac{2N(2N+1)!(2N)!}{16^N(2N-1)N!^3(N+1)!}. \tag{B.25}$$

For large N, the Stirling approximation can be used for the factorials and equation (B.25) reduces to

$$\left(\frac{\mathrm{d}k_1}{\mathrm{d}a}\right)_{a=0} = \frac{2}{N}\left[1 - \frac{1}{4N} + \frac{17}{32N^2} - \frac{47}{128N^3} + O\left(\frac{1}{N^4}\right)\right]; \tag{B.26}$$

therefore for $N \to \infty$, $\left(\frac{\mathrm{d}k_1}{\mathrm{d}a}\right)_{a=0} = 0$.

Appendix C

In this appendix we provide the asymptotic behaviour of the second derivative of k_1 with respect to a at threshold, in the two opposite limits $a \to 0$ and $a \to +\infty$. Deriving equation (29), one gets

$$\frac{\mathrm{d}^2 k_1}{\mathrm{d}a^2} = -\frac{1}{\frac{\partial \det A}{\partial k_1}}\frac{\partial^2 \det A}{\partial a^2} - \frac{\left(\frac{\partial \det A}{\partial a}\right)^2}{\left(\frac{\partial \det A}{\partial k_1}\right)^3}\frac{\partial^2 \det A}{\partial k_1^2} + 2\frac{\frac{\partial \det A}{\partial a}}{\left(\frac{\partial \det A}{\partial k_1}\right)^2}\frac{\partial^2 \det A}{\partial a \partial k_1}, \tag{C.1}$$

where the second derivative of $\det A$ in order to a variable is equal to the sum of N determinants in which one row (or column) has been substituted by the second derivative plus twice the sum of determinants in which two rows (or columns) have been substituted by the first derivative.

Let us consider first the case of a zero-size parameter. The first term to be evaluated is $\frac{\partial^2 \det A}{\partial a^2}$. In this limit, the second derivative with respect to a of the matrix elements is zero; therefore, the first sum of determinants is also equal to zero. Since the first row of A at threshold is identically zero, the only terms that survive in the second sum of determinants are those in which the first row is the derivatives of the matrix elements leading to

$$\frac{\partial^2 \det A}{\partial a^2} = 2\sum_{l=2}^{N} \det Z_l \tag{C.2}$$

with

$$Z_l(j,m) = (\delta_{j,1} + \delta_{j,l})\frac{\partial A_{j,m}}{\partial a} + (1-\delta_{j,1})(1-\delta_{j,l})A_{j,m}. \tag{C.3}$$

Substituting the value of the derivatives of the matrix elements of A

$$\frac{\partial A^{\pm}_{jm}}{\partial a} = -z_m^2\left(1 + f_m^{\pm 2}(z_m a)\right)o_{jm}, \tag{C.4}$$

which in our case reduce to

$$\left.\frac{\partial A_{j,m}}{\partial a}\right|_{a=0} = -\pi^2(1-(m-1/2)^2)o_{j,m}; \tag{C.5}$$

the determinant of Z_l becomes

$$\det Z_l = \pi^{N+2}\left[\prod_{i=2}^{N}\sqrt{i^2-1}\right]\frac{1}{\sqrt{l^2-1}}\det\left\|\delta_{j,1}+\delta_{j,l}\frac{o_{l,m}}{o_{1,m}}+(1-\delta_{j,1})(1-\delta_{j,l})o_{j,m}\right\| \tag{C.6}$$

leading to

$$\begin{aligned}\det Z_l &= (2-2l^2)\frac{4^{N^2-N}(2N+1)!!(2N-3)!!}{N!(N+1)!(N-1)!}\prod_{t=1,N}\frac{(2t-1)!^2}{(4t-1)!!(4t-3)!!}\\ &= (2-2l^2)\frac{(2N+1)!!(2N-3)!!}{4^N(N+1)!(N-1)!}\det O.\end{aligned} \tag{C.7}$$

Combining the previous results, we obtain

$$\frac{\partial^2\det A}{\partial a^2} = -\pi^{N+2}\left[\sum_{l=2}^{N}\sqrt{l^2-1}\right]\sqrt{\frac{N+1}{2N}}\frac{(2N+1)!!(2N-3)!!}{4^{N-1}(N+1)(N-1)!}\det O. \tag{C.8}$$

The ratio appearing in the first term of equation (C.1), making use of equations (B.19) and (C.8), reduces to

$$-\frac{\frac{\partial^2\det A}{\partial a^2}}{\frac{\partial\det A}{\partial k_1}} = \frac{\pi^2(2N+1)!!(2N-1)!!}{4^{N-1}(2N-1)(N+1)!(N-1)!}\sum_{l=2}^{N}\sqrt{l^2-1}. \tag{C.9}$$

The second term of equation (C.1) contains the second derivative of $\det A$ with respect to k_1. Since for $k_1 = a = 0$ the matrix A and the second derivative of the matrix with respect to k_1 have the first row equal to zero, while the first derivative is different from zero only in the first row, this term is zero.

The last contributions still missing in the calculation of equation (C.1) are the mixed derivatives of $\det A$ with respect to a and k. But the second derivative of a determinant with respect to two variables, is equal to the sum of N determinants in which one row (or column) has been substituted by the second derivative, plus the sum of determinants in which two rows (or columns) have been substituted by the first derivative, one of them with respect to the first variable, and the other with respect to the second one. Since the mixed second derivative of the matrix elements is equal to zero, the first sum is zero. For the second sum, since the first row of the matrix A is identically zero, and the derivative with respect to k is different from zero only for the first row, the only term that survives is the one where the first row is derived with respect to k and the other with respect to a, that is

$$\frac{\partial^2\det A}{\partial a\partial k_1} = \sum_{l=2}^{N}\det\left\|\delta_{j,1}\frac{\partial A_{j,m}}{\partial k_1}+\delta_{j,l}\frac{\partial A_{j,m}}{\partial a}+(1-\delta_{j,1})(1-\delta_{j,l})A_{j,m}\right\|. \tag{C.10}$$

Using equations (C.5) and (B.1), we obtain

$$\begin{aligned}\frac{\partial^2\det A}{\partial a\partial k_1} &= 4^{N^2}\pi^{N+1}\sqrt{\frac{N+1}{2N}}\prod_{t=1}^{N}\frac{(2t-1)!^2}{(4t-3)!!(4t-1)!!}\cdot\sum_{l=2}^{N}\sqrt{l^2-1}\\ &\quad\times\left[1-2^{1-2N}\frac{l^2}{(l-1)(l+1)}\frac{(2N-2l-1)!!(2N+2l-1)!!}{(N-l)!(N+l)!}\right].\end{aligned} \tag{C.11}$$

Combining all the previous results we finally find for equation (C.1)

$$\frac{\mathrm{d}^2k_1}{\mathrm{d}a^2} = 8\pi^2\frac{(2N-3)!!(2N+1)!!}{16^N(N-1)!(N+1)!}\sum_{m=2}^{N}\frac{m^2(2N-2m-1)!!(2N+2m-1)!!}{\sqrt{m^2-1}(N-m)!(N+m)!}. \tag{C.12}$$

The value of this expression for very large N can be inferred through the following argument. One first rewrites the double factorials in terms of binomial coefficients, and expands the troublesome weight factor $m^2/\sqrt{m^2-1}$ in a power series, to get

$$\frac{\mathrm{d}^2 k_1}{\mathrm{d}a^2} = \sum_{l=0}^{\infty} \mathcal{C}(l, N) \tag{C.13}$$

where

$$\mathcal{C}(l, N) = \binom{2l}{l} \frac{1}{4^l} \frac{8\pi^2}{16^{2N}} \frac{N(2N+1)}{(N+1)(2N-1)} \binom{2N}{N}^2 \sum_{m=2}^{N} m^{1-2l} \binom{2N-2m}{N-m} \binom{2N+2m}{N+m}. \tag{C.14}$$

Using the identity

$$\sum_{m=1}^{N} m \binom{2N-2m}{N-m} \binom{2N+2m}{N+m} = \frac{1}{2}(2N-1)(N+1) \binom{2N-2}{N-1} \binom{2N+2}{N+1} \tag{C.15}$$

and the Stirling approximation for the binomial coefficients, one finds that $\mathcal{C}(0, N)$ behaves for large N as

$$\mathcal{C}(0, N) \sim 4 \frac{(2N+1)^2 (N-1)(2N+3)}{(N+1)^2 (2N-1)^2}. \tag{C.16}$$

One may thus conclude that $\lim_{N\to\infty} \mathcal{C}(0, N) = 8$.

To complete our argument, we have to show that all other terms in the series expansion (C.13) go to zero as $N \to \infty$. This can be proved by bounding from above each term in equation (C.13) with a quantity, which vanishes for $N \to \infty$. Let us consider, for instance, the term $\mathcal{C}(1, N)$. Resorting to the Stirling approximation for $\binom{2N+2m}{N+m}$, and taking into account that $m \geqslant 2$, one has

$$\frac{2^{2N}}{\sqrt{\pi N}} \sum_{m=2}^{N} \frac{2^{2m}}{2m} \binom{2N-2m}{N-m} < \frac{2^{2N-2}}{\sqrt{\pi N}} \sum_{m=2}^{N} 2^{2m} \binom{2N-2m}{N-m}. \tag{C.17}$$

The sum in equation (C.17) can be performed with the aid of the identity

$$\sum_{m=2}^{N} 2^{2m} \binom{2N-2m}{N-m} = 16(2N-3) \binom{2N-4}{N-2}. \tag{C.18}$$

Using again Stirling's formula for the binomial coefficient $\binom{2N-4}{N-2}$, one finally has that $\mathcal{C}(1, N)$ is bounded from above by the quantity

$$\frac{2(2N+1)}{(N+1)\sqrt{N(N-2)}}$$

which approaches 0 as $N \to \infty$. Similar considerations apply to the higher-order terms in equation (C.13), so that one may conclude that $\frac{\mathrm{d}^2 k_1}{\mathrm{d}a^2} = 8$ when an infinite number of basis functions are included in the calculation.

Finally, we have to obtain the second derivative of k_1 for a large-size parameter where a bound state appears. This is obviously done approximatively. We take for a the expression given by equation (A.5), which corresponds to the first-order correction of the solution.

From the general expression of equation (C.1), the derivatives of the det A in order to a and k_1 have to be determined. Using equations (A.3) and (A.4) for the matrix elements, and

the properties of determinants, noting that only the first column of the second derivative is different from zero, leading to only one term in the sum of determinants, we obtain

$$\frac{\partial^2 \det A}{\partial a^2} = -2 \det B \left(\left(\frac{\det B}{\det C} \right)^2 + \frac{3}{4}\pi^2 \right) \det C, \tag{C.19}$$

and

$$-\frac{\frac{\partial^2 \det A}{\partial a^2}}{\frac{\partial \det A}{\partial k_1}} = 2 \det B \frac{\left(\left(\frac{\det B}{\det C} \right)^2 + \frac{3}{4}\pi^2 \right) \det C}{\pi \det C + \frac{4}{3\pi} \frac{(\det B)^2}{\det C}} = \frac{3}{2}\pi \det B. \tag{C.20}$$

For the mixed derivative, since the second derivative with respect to a and k_1 of the matrix elements is zero, the only term that contributes is the double sum of determinants of matrices, where the row labelled by the first summation index is derived with respect to k_1, the column labelled by the second summation index is derived with respect to a, and the intersection between this row and column is derived with respect to k_1 and a. Noting that the derivative with respect to k_1 is only different from zero for the first row, and the derivative with respect to a is different from zero only for the first column we get

$$\frac{\partial^2 \det A}{\partial k_1 \partial a} = -\pi \left(\left(\frac{\det B}{\det C} \right)^2 + \frac{3}{4}\pi^2 \right) \det K \tag{C.21}$$

with

$$\begin{aligned} K_{j,m} = {} & ((1-\delta_{m,1})(1-\delta_{j,1})\pi(\sqrt{j^2-1} + \sqrt{(m-1/2)^2-1}) + (1-\delta_{m,1})\delta_{j,1} \\ & + (1-\delta_{j,1})\delta_{m,1})o_{j,m}. \end{aligned} \tag{C.22}$$

Combining the previous results

$$2\frac{\partial^2 \det A}{\partial k_1 \partial a} \frac{\frac{\partial \det A}{\partial a}}{\left(\frac{\partial \det A}{\partial k_1} \right)^2} = \frac{9}{8}\pi^3 \frac{\det K}{\det C}. \tag{C.23}$$

The last term to complete equation (C.1) is the second derivative of the matrix with respect to k_1, where the only contribution comes from the sum of determinants with the second derivative

$$\frac{\partial^2 \det A}{\partial k_1^2} = \frac{4}{3}\left(a \left[\left(\frac{\det B}{\det C} \right)^2 + \frac{3}{4}\pi^2 \right] + \frac{\det B}{\det C} \right) \det C + \sum_{l=1}^{N} \det M^l \tag{C.24}$$

with

$$\begin{aligned} M^l_{j,m} = o_{j,m} \Bigg(& \delta_{m,l} \left[(1-\delta_{j,1}) \frac{\pi}{\sqrt{j^2-1}} + (1-\delta_{m,1}) \frac{\pi}{\sqrt{(m-1/2)^2-1}} \right] \\ & + (1-\delta_{m,l}) \left(\pi\sqrt{j^2-1} - \delta_{m,1} \frac{\det B}{\det C} + \pi(1-\delta_{m,1})\sqrt{(m-1/2)^2-1} \right) \Bigg) \end{aligned} \tag{C.25}$$

and

$$\begin{aligned} -\frac{\left(\frac{\partial \det A}{\partial a} \right)^2}{\left(\frac{\partial \det A}{\partial k_1} \right)^3} \frac{\partial^2 \det A}{\partial k_1^2} = {} & -\left(\frac{3}{4}\pi \right)^2 \frac{1}{\det C \frac{4}{3\pi} \left(\left(\frac{\det B}{\det C} \right)^2 + \frac{3}{4}\pi^2 \right)} \\ & \times \left[\frac{4}{3} \left(a \left[\left(\frac{\det B}{\det C} \right)^2 + \frac{3}{4}\pi^2 \right] + \frac{\det B}{\det C} \right) \det C + \sum_{l=1}^{N} \det M^l \right] \end{aligned}$$

$$= -\frac{9}{16}\pi^3 a - \frac{9}{16}\pi^3 \frac{\det B}{\det C} \frac{1}{\left(\frac{\det B}{\det C}\right)^2 + \frac{3}{4}\pi^2}$$
$$- \left(\frac{3}{4}\pi\right)^2 \frac{1}{\det C \frac{4}{3\pi}\left(\left(\frac{\det B}{\det C}\right)^2 + \frac{3}{4}\pi^2\right)} \sum_{l=1}^{N} \det M^l. \tag{C.26}$$

Combining equations (C.20), (C.23) and (C.26), we obtain the final result

$$\frac{\mathrm{d}^2 k_1}{\mathrm{d}a^2} = -\frac{3}{16}\sqrt{3}\pi^3 n + 0.577\,482\,652\,977\,66(1) + \mathcal{O}\left(\mathrm{e}^{-\pi\sqrt{\frac{5}{3}}n}\right) \qquad n = 0, 1, 2, \ldots \tag{C.27}$$

valid for large a, and $N \to \infty$.

References

[1] van Wees B J, van Houten H, Beenakker C W J, Williamson J G, Kouwenhoven L P, van der Marel D and Foxon C T 1988 *Phys. Rev. Lett.* **60** 848
[2] Wharam D A, Thornton T J, Newbury R, Pepper M, Ahmed H, Frost J E F, Hasko D G, Peacock D C, Ritchie D A and Jones G A C 1988 *J. Phys. C: Solid State Phys.* **21** L209
[3] Appenzeller J, Schroer Ch, Shäpers Th, v d Hart A, Förster A, Lengeler B and Lüth H 1996 *Phys. Rev.* B **53** 9959
[4] Debray P, Raichev O E, Vasilopoulos P, Rahman M, Perrin R and Mitchell W C 2000 *Phys. Rev.* B **61** 10950
[5] Behringer R, Timp G, Baranger H U and Cunningham J E 1991 *Phys. Rev. Lett.* **66** 930
[6] Wu J C, Wybourne M N, Yindeepol W, Weisshaar A and Goodnick S M 1991 *Appl. Phys. Lett.* **59** 102
[7] Thornton T J 1995 *Rep. Prog. Phys.* **578** 311
[8] Smith C G 1996 *Rep. Prog. Phys.* **59** 235
[9] Londergan J T, Carini J P and Murdock D P 1999 *Binding and Scattering in Two-Dimensional Systems* (*Lecture Notes in Physics* vol m60) (Berlin: Springer)
[10] Ihn T 2004 *Electronic Quantum Transport in Mesoscopic Semiconductor Structures* (*STMP* vol 192) (New York: Springer)
[11] Datta S 1995 *Electronic Transport in Mesoscopic Systems* (Cambridge: Cambridge University Press)
[12] Wang J and Guo H 1993 *Phys. Rev.* B **48** 12072
[13] Pavlov B S, Popov I Yu and Frolov S V 2001 *Eur. Phys. J.* B **21** 283
[14] Kunze Ch 1993 *Phys. Rev.* B **48** 14338
[15] Hirayama Y, Tokura Y, Wieck A D, Koch S, Haug R J, von Klitzing K and Ploog K 1993 *Phys. Rev.* B **48** 7991
[16] Exner P, Šeba P, Tater M and Vˇanek D 1996 *J. Math. Phys.* **37** 4867
[17] Exner P and Vugalter S A 1996 *Ann. Inst. H Poincaré* **65** 109
[18] Exner P and Vugalter S A 1997 *J. Phys. A: Math. Gen.* **30** 7863
[19] Borisov D, Exner P and Gadyl'shin R 2002 *J. Math. Phys.* **43** 6265
[20] Popov I Yu 1999 *Rep. Math. Phys.* **43** 427
[21] Popov I Yu 2001 *Appl. Math. Lett.* **14** 109
[22] Gadyl'shin R R 2004 *C. R. Mecanique* **332** 647
[23] Linton C M and Ratcliffe K 2004 *J. Math. Phys.* **45** 1359
[24] Press W H, Teukolsky S A, Vetterling W T and Flannery B P 1992 *Numerical Recipes* 2nd edn (Cambridge: Cambridge University Press) pp 718–26